

Dalton Transactions

Accepted Manuscript



This is an *Accepted Manuscript*, which has been through the Royal Society of Chemistry peer review process and has been accepted for publication.

Accepted Manuscripts are published online shortly after acceptance, before technical editing, formatting and proof reading. Using this free service, authors can make their results available to the community, in citable form, before we publish the edited article. We will replace this *Accepted Manuscript* with the edited and formatted *Advance Article* as soon as it is available.

You can find more information about *Accepted Manuscripts* in the [Information for Authors](#).

Please note that technical editing may introduce minor changes to the text and/or graphics, which may alter content. The journal's standard [Terms & Conditions](#) and the [Ethical guidelines](#) still apply. In no event shall the Royal Society of Chemistry be held responsible for any errors or omissions in this *Accepted Manuscript* or any consequences arising from the use of any information it contains.

ARTICLE

Near-infrared (NIR) emitting Nd/Yb(III) complexes sensitized by MLCT states of Ru(II)/Ir(III) metalloligands in visible light region

Cite this: DOI: 10.1039/x0xx00000x

Received 00th January 2012,
Accepted 00th January 2012

DOI: 10.1039/x0xx00000x

www.rsc.org/Lu-Yin Zhang^a, Ya-Jun Hou^a, Mei Pan^{a,b*}, Ling Chen^a, Yi-Xuan Zhu^a, Shao-Yun Yin^a, Guang Shao^{a,*}, and Cheng-Yong Su^{a,c,*}

Four Ru(II)/Ir(III) metalloligands have been designed and synthesized from polypyridine and bibenzimidazole (BiBzIm) organic ligands, which show strong visible light absorption via metal-to-ligand charge transfer (MLCT) transitions. Nd/Yb(III) complexes were further assembled from these Ru(II)/Ir(III) metalloligands, and Ln(III)-centered NIR emissions can be efficiently sensitized by ³MLCT states of the metalloligands in visible-light region. The energy transfer rates for the complexes are generally in the order Nd > Yb, which is due to the better matching between ³MLCT states of Ru(II)/Ir(III) metalloligands and densely distributed excited states of Nd(III) ions. Long decayed lifetimes in μs scale and high quantum yields up to 1% are obtained in these lanthanide complexes, suggesting that the Ru(II)/Ir(III) metalloligands can serve as good visible light harvesting antenna to efficiently sensitize Ln(III)-based NIR luminescence.

Introduction

Lanthanide ions possess characteristic luminescence with high color purity and long lifetimes, therefore have long been the focus of scientists' research for potential applications in such fields as chemical analysis, cell imaging, immunoassay, organic electroluminescence, optical communication, and so on.¹⁻³ Especially, the near-infrared (NIR) photoluminescence of Ln(III) ions such as Pr^{III}, Nd^{III}, Er^{III} and Yb^{III} is transparent to biological tissue which allows imaging through relatively thick tissue samples. Therefore, NIR emitting lanthanides offer major advantages for applications in biological luminescent imaging agents and bioprobes.^{4,5} However, the f-f transitions of lanthanide ions are usually forbidden, which results in low absorption cross section and poor luminescence efficiency which limits their efficient application. In recent decades, organic ligands are introduced to assemble lanthanide coordination complexes to obtain highly efficient lanthanide luminescence via so called Antenna effect. In which, the organic ligands efficiently absorb the light like an antenna, followed by energy transfer to the excited states of lanthanide ions. When the lanthanide ions return to the ground state via radiative transitions, characteristic fluorescence of the lanthanide is produced.^{6,7} Up to now, abundant lanthanide complexes with either visible or NIR emissions have been designed and synthesized from various types of organic ligands.^{8,9} However, since most of the organic chromophores can only be excited under UV light by $\pi \rightarrow \pi^*$ transitions with relatively high energy, luminescent lanthanide complexes which can

be excited by visible light in the lower energy region remain relatively rare. This limits the application of most lanthanide complexes to some extent, especially in such fields as bio-imaging, since UV excitation will inevitably cause some damages to the bio-systems.^{10,11}

Alternatively, metalloligands incorporating *d*-block chromophores (such as Ir^{III}, Ru^{II}, Pt^{II}, Au^I, et al) have wider absorption bands ranging from UV to visible and even near-infrared region, contributed by both $\pi\pi^*$ transitions of the organic parts and MLCT (metal-to-ligand charge transfer) transitions involving the *d*-block metals such as Ru^{II} or Ir^{III}.¹²⁻¹⁴ Therefore, coordination complexes assembled from such metalloligands can meet the requirement of visible-light excitation with obvious advantages over UV excitation, especially in the application of non-invasive bio-analysis and bio-imaging. Furthermore, the low ³MLCT excited states of the metalloligands can better fit the excited energy levels of near-infrared (NIR) emitting Ln(III) ions, which usually reside below 20,000 cm⁻¹.¹⁵⁻¹⁷ Therefore, the design and assembly of lanthanide coordination complexes from *d*-block metalloligands have become a hot topic in recent years.^{18,19} Herein, we designed a series of Ru(II)/Ir(III) polypyridine metalloligands to sensitize the NIR luminescence of Nd(III) and Yb(III) successfully by excitation wavelength in the visible region (≥ 400 nm). The *d*→*f* energy transfer rates from different Ru(II)/Ir(III) metalloligands to Ln(III) centers are analysed by

intensive luminescent lifetime study to better understand the fundamental energy transfer processes in the complexes.

Experimental

Materials and methods

All experimental materials were of AR grade and used as purchased without further purification. The ^1H NMR spectra were recorded on Bruker Avance 400 NMR spectrometer using TMS as the internal standard. The HR-ESI-TOF-MS spectra were detected on Bruker maXis 4G ESI-Q-TOF. The C, H, and N elemental analyses were performed on Perkin-Elmer 240 elemental analyzer. The UV-vis absorption spectra were measured on SHIMADZU UV-3150 UV-Vis-NIR Spectrophotometer. Photoluminescence spectra were measured on EDINBURGH FLS980 fluorescence spectrophotometer.

Syntheses of metalloligands

1H,1'H-2,2'-bibenzo[d]imidazole (BiBzImH₂): A mixture of *o*-phenylenediamine dihydrochloride (1.79 g, 10 mmol) and oxalic acid dihydrate (0.567 g, 4.5 mmol) in 10 ml ethylene glycol (EG) was heated to 150 °C and reacted for 24 hours, and then cooled to room temperature. The reaction mixture was poured into 100 ml water, and the pH value was adjusted to 10. The precipitates were filtered and washed with water until the pH value reached 7, and then dried to get yellowish product BiBzImH₂. Yield: 68%. ^1H NMR (400 MHz, DMSO-*d*₆, 25 °C): δ = 13.53 (s, 2H), 7.77 (d, 2H), 7.56 (d, 2H), 7.30 (m, 4H).

Ru(bpy)₂Cl₂·2H₂O: 1.56 g (5.96 mmol) RuCl₃·3H₂O was dissolved in 10 ml DMF, and then 1.68 g (0.4 mmol) LiCl and 1.87 g (12 mmol) 2,2'-bipyridine were added. The mixture was refluxed at 145 °C under the protection of N₂ for 8 hours and then cooled to room temperature. 50 ml acetone was added into the reaction mixture and frozen at 0 °C overnight. Purple black precipitates were obtained by filtration, which was washed with small amounts of cooled water, and then washed successively with 5 ml methanol and 20 ml ethyl ether. The final product of Ru(bpy)₂Cl₂·2H₂O was obtained after drying in vacuum. Yield: 63%. ^1H NMR (400 MHz, DMSO-*d*₆, 25 °C): δ = 9.96 (d, 2H), 8.85 (d, 2H), 8.50 (d, 2H), 8.08 (t, 2d), 7.78 (t, 2H), 7.68 (t, 2H), 7.50 (d, 2H), 7.12 (t, 2H).

[Ru(bpy)₂(BiBzImH₂)](PF₆)₂ [L_{Ru}·(PF₆)₂]: 0.52 g (1 mmol) Ru(bpy)₂Cl₂·2H₂O and 0.33 g (1.4 mmol) BiBzImH₂ were added into 14 ml ethylene glycol (EG), which was refluxed under the protection of N₂ for 3 hours and then cooled to room temperature. The reaction solution was filtered, then 100 ml water and 2 ml HCl was added into the filtrate. Then saturated solution of KPF₆ was added to get red precipitate, which was stirred for a while and then filtered. The final crimson product of LRu·(PF₆)₂ was obtained after washing with water for several times and then drying in vacuum. Yield: 70%. ^1H NMR (400 MHz, DMSO-*d*₆, 25 °C): δ = 8.86 (d, 2H), 8.76 (d, 2H), 8.25 (t, 2H), 8.07 (t, 2H), 8.00 (d, 2H), 7.89 (m, 4H), 7.61 (t, 2H), 7.48 (t, 2H), 7.40 (t, 2H), 7.07 (t, 2H), 5.64 (d, 2H). ^{13}C NMR (400 MHz, DMSO-*d*₆, 25 °C): δ = 159.03, 157.33, 152.80, 152.60, 142.00, 138.06, 137.50, 128.34, 127.89, 126.03, 125.13, 124.62,

124.33, 115.54, 114.94. ESI⁺-MS: m/z = 647.1180 ([L_{Ru}·2PF₆⁻-H⁺]⁺, calc. 647.1249).

Ru(phen)₂Cl₂·2H₂O: Ru(phen)₂Cl₂·2H₂O was obtained by the similar procedure to Ru(bpy)₂Cl₂·2H₂O unless phenanthroline (phen) was used instead of 2,2'-bipyridine. Yield: 70%. ^1H -NMR (400 MHz, DMSO-*d*₆, 25 °C): δ = 10.30 (d, 2H), 8.74 (d, 2H), 8.30 (d, 2H), 8.24 (m, 4H), 8.16 (d, 2H), 7.77 (d, 2H), 7.34 (t, 2H).

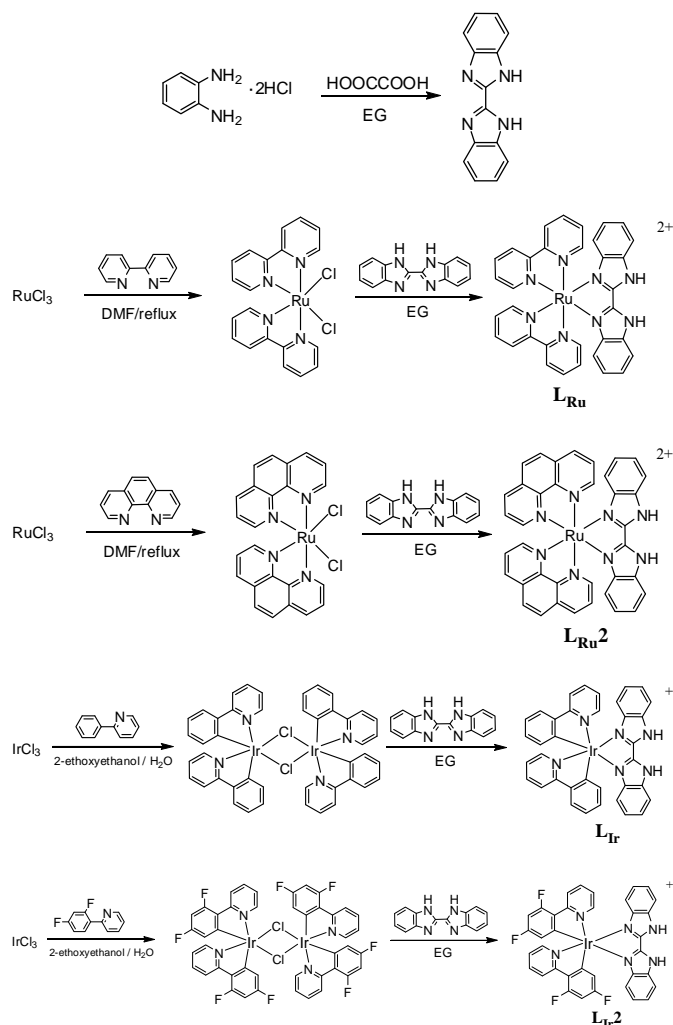
[Ru(phen)₂(BiBzImH₂)](PF₆)₂ [L_{Ru}2·(PF₆)₂]: L_{Ru}2·(PF₆)₂ was obtained by the similar procedure to LRu·(PF₆)₂ unless Ru(phen)₂Cl₂·2H₂O was used instead of Ru(bpy)₂Cl₂·2H₂O. Yield: 92%. ^1H -NMR (400 MHz, DMSO-*d*₆, 25 °C): δ = 8.81 (d, 2H), 8.73 (d, 2H), 8.35 (m, 6H), 8.27 (d, 2H), 7.81 (m, 6H), 7.28 (t, 2H), 6.86 (t, 2H), 5.31 (d, 2H). ^{13}C NMR (400 MHz, DMSO-*d*₆, 25 °C): δ = 154.09, 153.98, 149.34, 148.25, 142.40, 136.81, 136.47, 130.58, 128.57, 128.25, 126.96, 126.36, 125.68, 124.82, 115.51, 114.71. ESI⁺-MS: m/z = 695.1450 ([L_{Ru}2·2PF₆⁻-H⁺]⁺, calc. 695.1250).

[Ir(ppy)₂Cl]₂: 0.25 g (0.7 mmol) IrCl₃·3H₂O and 270 μL (1.9 mmol) 2-phenylpyridine (ppy) were added into a mixture of 2-ethoxyethanol/water (30 ml, v:v=3:1), and then reacted at 120 °C under the protection of N₂ for 24 hours and then cooled to room temperature. Precipitates were obtained by filtration, which was washed with water. Yellow product of [Ir(ppy)₂Cl]₂ was obtained after drying (yield: 70%). ^1H NMR (400 MHz, DMSO-*d*₆, 25 °C): δ = 9.81 (d, 2H), 9.55 (d, 2H), 8.28 (d, 2H), 8.20 (d, 2H), 8.11 (t, 2H), 8.02 (t, 2H), 7.81 (d, 2H), 7.75 (d, 2H), 7.58 (t, 2H), 7.46 (t, 2H), 6.91 (t, 2H), 6.85 (t, 2H), 6.78 (t, 2H), 6.70 (t, 2H), 6.27 (d, 2H), 5.68 (d, 2H).

[Ir(ppy)₂(BiBzImH₂)]Cl (L_{Ir}·Cl): 0.608 g (0.5 mmol) [Ir(ppy)₂Cl]₂ and 0.234 g (1 mmol) BiBzImH₂ were added into 20 ml ethylene glycol (EG), which was reacted at 65 °C under the protection of N₂ for 24 hours and then filtered. Light green product of L_{Ir}·Cl was obtained after washing with water for several times and then drying. Yield: 79%. ^1H NMR (400 MHz, DMSO-*d*₆, 25 °C): δ = 8.20 (d, 2H), 7.93 (d, 2H), 7.84 (m, 4H), 7.77 (d, 2H), 7.38 (t, 2H), 7.10 (m, 4H), 7.02 (t, 2H), 6.94 (t, 2H), 6.38 (d, 2H), 6.14 (d, 2H). ^{13}C NMR (400 MHz, DMSO-*d*₆, 25 °C): δ = 167.71, 150.12, 148.67, 145.43, 140.62, 138.58, 132.23, 129.86, 125.78, 125.09, 124.83, 124.11, 122.34, 119.81, 116.88, 114.89. ESI⁺-MS: m/z = 735.2124 ([L_{Ir}]⁺, calc. 735.1844).

[Ir(Fppy)₂Cl]₂: 0.604 g (1.7 mmol) IrCl₃·3H₂O and 0.719 g (3.7 mmol) 2-(2,4-difluorophenyl)pyridine (Fppy) were added into a mixture of 2-ethoxyethanol/water (30 ml, v:v=3:1), and then reacted at 120 °C under the protection of N₂ for 24 hours and then cooled to room temperature. 10 ml water was added to adjust the pH value of the reaction mixture. Precipitates were obtained by filtration, which was washed with small amounts of EtOH and ethyl ether, and then large amounts of *n*-hexane. Yellow product of [Ir(Fppy)₂Cl]₂ was obtained after drying (yield: 80%), which was applied directly into the next procedure without further characterization due to its insolubility in common organic solvents.

[Ir(Fppy)₂(BiBzImH₂)]·Cl (L_{Ir}·2·Cl): L_{Ir}·2·Cl was obtained by the similar procedure to L_{Ir}·Cl unless [Ir(Fppy)₂Cl]₂ was used instead of [Ir(ppy)₂Cl]₂. Yield: 68%. ¹H NMR (400 MHz, DMSO-*d*₆, 25 °C): δ = 8.26 (d, 2H), 7.96 (t, 2H), 7.83 (d, 2H), 7.78 (d, 2H), 7.40 (t, 2H), 7.16 (m, 4H), 7.06 (t, 2H), 6.20 (d, 2H), 5.81 (d, 2H). ¹³C NMR (400 MHz, DMSO-*d*₆, 25 °C): δ = 163.51, 163.44, 150.85, 140.25, 139.96, 129.20, 126.08, 125.35, 124.88, 124.65, 123.35, 123.15, 116.07, 115.27, 114.25, 114.09, 99.41, 99.14. ESI⁺-MS: m/z = 807.1912 ([L_{Ir}·2]⁺, calc. 807.1468).



Scheme 1 Synthetic route of Ru(II)/Ir(III) metalloligands.

Syntheses of lanthanide complexes

Ln(tta)₃(H₂O)₂ (Ln = Nd, Yb or Gd): 0.667 g (3 mmol) 2-thenoyltrifluoroacetone (Htta) was dissolved in 15 ml EtOH, and then 1 mol/l HCl was added to adjust the pH value to 6-7. Then 0.358 g (1 mmol) NdCl₃·6H₂O, 0.387 g (1 mmol) YbCl₃·6H₂O or 0.372 g (1 mmol) GdCl₃·6H₂O was dissolved in 5 ml water and added into the solution of Htta. Then 100 ml water was added into the mixture and stirred at 60 °C for 2 hours and then cooled to room temperature. Precipitates were obtained by filtration, which was washed with water and dried in vacuum.

L_{Ru}-Nd(tta)₃: 0.38 g (0.4 mmol) L_{Ru}·(PF₆)₂ and 0.34 g (0.4 mmol)

Nd(tta)₃(H₂O)₂ were added into 7 ml CH₂Cl₂ (DCM), and then 1 ml triethylamine (Et₃N) was added dropwisely into the mixture and stirred for 10 minutes under room temperature. Then 5 ml *n*-hexane was added into the reaction solution and stirred for 2 minutes. The final product of L_{Ru}-Nd(tta)₃ was obtained after filtration and washed with *n*-hexane and then dried naturally. Yield: 83%. ESI⁺-MS: m/z = 1453.9939 ([L_{Ru}-Nd(tta)₃-H⁺]⁺, calc. 1454.0011). Anal. Calc. (%) for C₇₀H₆₈F₂₁N₁₀O₆P₂RuS₃Nd (L_{Ru}-Nd(tta)₃+2Et₃N+2H⁺+2PF₆): C, 43.18; H, 3.52; N, 7.20. Found: C, 43.41; H, 3.23; N, 7.47 %. ¹H-NMR (400 MHz, DMSO-*d*₆, 25 °C): δ = 8.80 (d, 2H), 8.70 (d, 2H), 8.16 (t, 2H), 7.98 (m, 4H), 7.78 (s, 2H), 7.55 (t, 4H), 7.44 (t, 2H), 7.01 (t, 2H), 6.72 (t, 2H), 5.48 (d, 2H). ¹³C NMR (400 MHz, DMSO-*d*₆, 25 °C): δ = 159.34, 157.71, 152.43, 151.63, 144.21, 136.69, 136.07, 127.60, 127.34, 124.21, 123.92, 121.73, 121.30, 117.38, 113.05, 46.05.

L_{Ru}-Yb(tta)₃: L_{Ru}-Yb(tta)₃ was obtained by the similar procedure to L_{Ru}-Nd(tta)₃ unless Yb(tta)₃(H₂O)₂ was used instead of Nd(tta)₃(H₂O)₂. Yield: 85%. ESI⁺-MS: m/z = 1484.0606 ([L_{Ru}-Yb(tta)₃-H⁺]⁺, calc. 1484.0695). Anal. Calc. (%) for C₇₀H₆₈F₂₁N₁₀O₆P₂RuS₃Yb (L_{Ru}-Yb(tta)₃+2Et₃N+2H⁺+2PF₆): C, 42.48; H, 3.47; N, 7.08. Found: C, 42.42; H, 3.60; N, 6.89 %. ¹H-NMR (400 MHz, DMSO-*d*₆, 25 °C): δ = 8.85 (d, 2H), 8.75 (d, 2H), 8.23 (t, 2H), 8.01 (m, 4H), 7.79 (d, 2H), 7.60 (t, 2H), 7.55 (d, 2H), 7.47 (t, 2H), 7.36 (s, 1H), 7.07 (t, 2H), 6.79 (t, 2H), 5.70 (s, 1H), 5.51 (d, 2H), 5.30 (s, 1H). ¹³C NMR (400 MHz, DMSO-*d*₆, 25 °C): δ = 159.31, 157.68, 152.61, 151.73, 151.43, 143.75, 137.06, 136.47, 132.60, 127.87, 127.49, 126.78, 124.32, 124.06, 122.65, 122.35, 113.54, 52.45, 46.11.

L_{Ru}-Gd(tta)₃: L_{Ru}-Gd(tta)₃ was obtained by the similar procedure to L_{Ru}-Nd(tta)₃ unless Gd(tta)₃(H₂O)₂ was used instead of Nd(tta)₃(H₂O)₂. Yield: 80%. ESI⁺-MS: m/z = 1468.0151 ([L_{Ru}-Gd(tta)₃-H⁺]⁺, calc. 1468.0152). Anal. Calc. (%) for C₇₀H₆₈F₂₁N₁₀O₆P₂RuS₃Gd (L_{Ru}-Gd(tta)₃+2Et₃N+2H⁺+2PF₆): C, 42.83 H, 3.47; N, 7.14. Found: C, 42.42; H, 3.32; N, 7.12 %.

L_{Ru2}-Nd(tta)₃: L_{Ru2}-Nd(tta)₃ was obtained by the similar procedure to L_{Ru}-Nd(tta)₃ unless L_{Ru2}·(PF₆)₂ was used instead of L_{Ru}·(PF₆)₂. Yield: 80%. ESI⁺-MS: m/z = 1502.0034 ([L_{Ru2}-Nd(tta)₃-H⁺]⁺, calc. 1502.0013). Anal. Calc. (%) for C₆₈H₅₃F₁₅N₉O₆PRuS₃Nd (L_{Ru2}-Nd(tta)₃+2Et₃N+2H⁺+2PF₆): C, 44.48; H, 3.41; N, 7.01. Found: C, 44.66; H, 3.28; N, 7.02 %. ¹H-NMR (400 MHz, DMSO-*d*₆, 25 °C): δ = 8.76 (d, 2H), 8.66 (d, 2H), 8.32 (m, 6H), 8.24 (d, 2H), 7.83 (m, 2H), 7.78 (m, 2H), 7.55 (d, 2H), 7.01 (t, 2H), 6.63 (t, 2H), 5.15(d, 2H). ¹³C NMR (400 MHz, DMSO-*d*₆, 25 °C): δ = 153.87, 153.04, 151.62, 149.74, 148.64, 135.89, 135.54, 130.47, 128.43, 128.14, 126.66, 126.13, 122.53, 122.32, 113.39, 46.08.

L_{Ru2}-Yb(tta)₃: L_{Ru2}-Yb(tta)₃ was obtained by the similar procedure to L_{Ru2}-Nd(tta)₃ unless Yb(tta)₃(H₂O)₂ was used instead of Nd(tta)₃(H₂O)₂. Yield: 85%. ESI⁺-MS: m/z = 1532.0263 ([L_{Ru2}-Yb(tta)₃-H⁺]⁺, calc. 1532.0296). Anal. Calc. (%) for C₆₈H₅₃F₁₅N₉O₆PRuS₃Yb (L_{Ru2}-Yb(tta)₃+Et₃N+H⁺+PF₆): C, 45.92; H, 3.01; N, 7.09. Found: C, 45.35; H, 3.22; N, 7.82 %. ¹H-NMR (400 MHz, DMSO-*d*₆, 25 °C): δ = 8.77 (d, 2H), 8.67 (d, 2H), 8.35 (m, 6H), 8.24 (d, 2H), 7.88 (m, 2H), 7.78 (m, 2H), 7.37(s), 7.52 (d, 2H), 7.00 (t, 2H), 6.62 (t, 2H), 5.71(s), 5.19(d, 2H). ¹³C NMR (400 MHz,

DMSO-*d*₆, 25 °C): δ 153.87, 153.04, 151.59, 149.75, 148.65, 144.09, 135.89, 135.55, 132.62, 130.48, 128.44, 128.16, 126.82, 126.66, 126.12, 122.52, 113.39, 46.18.

L_{Ru2}-Gd(tta)₃: L_{Ru2}-Gd(tta)₃ was obtained by the similar procedure to L_{Ru2}-Nd(tta)₃ unless Gd(tta)₃(H₂O)₂ was used instead of Nd(tta)₃(H₂O)₂. Yield: 82%. ESI⁺-MS: *m/z* = 1516.0160 ([L_{Ru2}-Gd(tta)₃-H⁺]⁺, calc. 1516.0153). Anal. Calc. (%) for C₆₈H₅₃F₁₅N₉O₆PRuS₃Gd (L_{Ru2}-Gd(tta)₃+Et₃N+H⁺+PF₆⁻): C, 44.20; H, 3.38; N, 6.97. Found: C, 43.77; H, 3.01; N, 7.29 %.

L_{Ir}-Nd(tta)₃: L_{Ir}-Nd(tta)₃ was obtained by the similar procedure to L_{Ru}-Nd(tta)₃ unless L_{Ir}-Cl was used instead of L_{Ru}-(PF₆)₂. Yield: 45%. Anal. Calc. for C₆₀H₃₆F₉N₆O₆S₃ClIrNd (L_{Ir}-Nd(tta)₃·Cl): C, 45.72; H, 2.30; N, 5.33. Found: C, 45.53; H, 3.45; N, 5.30 %. ¹H-NMR (400 MHz, DMSO-*d*₆, 25 °C): δ = 8.14 (d, 2H), 7.89 (d, 2H), 7.77 (t, 4H), 7.67 (d, 2H), 7.54 (d, 2H), 7.07 (m, 4H), 6.89 (t, 2H), 6.76 (t, 2H), 6.43 (d, 2H), 6.02 (d, 2H). ¹³C NMR (400 MHz, DMSO-*d*₆, 25 °C): δ = 99.99, 46.21.

L_{Ir}-Yb(tta)₃: L_{Ir}-Nd(tta)₃ was obtained by the similar procedure to L_{Ir}-Nd(tta)₃ unless Yb(tta)₃(H₂O)₂ was used instead of Nd(tta)₃(H₂O)₂. Yield: 39%. Anal. Calc. for C₆₆H₅₁F₉N₇O₆S₃ClIrYb (L_{Ir}-Yb(tta)₃·Et₃N·Cl): C, 46.46; H, 3.01; N, 5.75. Found: C, 45.32; H, 3.55; N, 5.80 %. ¹H-NMR (400 MHz, DMSO-*d*₆, 25 °C): δ = 8.13 (d, 2H), 7.87 (d, 2H), 7.77 (t, 4H), 7.67 (d, 2H), 7.53 (d, 2H), 7.37(s), 7.05 (m, 4H), 6.88 (t, 2H), 6.74 (t, 2H), 6.42 (d, 2H), 6.02 (d, 2H), 5.71(s), 5.62(s), 5.30(s). ¹³C NMR (400 MHz, DMSO-*d*₆, 25 °C): δ = 168.31, 151.83, 151.69, 149.36, 145.55, 137.84, 132.49, 129.51, 126.80, 124.86, 124.12, 123.55, 122.41, 122.17, 121.52, 119.49, 115.71, 46.08.

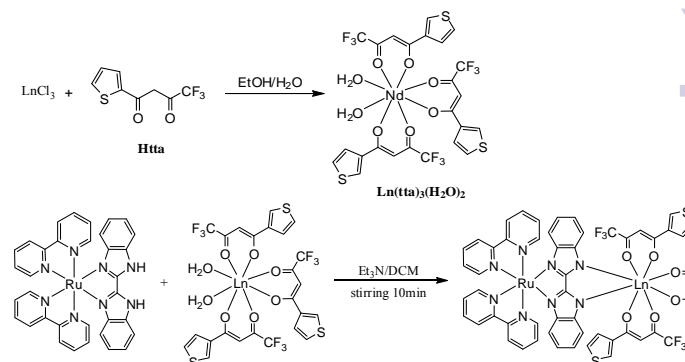
L_{Ir}-Gd(tta)₃: L_{Ir}-Gd(tta)₃ was obtained by the similar procedure to L_{Ir}-Nd(tta)₃ unless Gd(tta)₃(H₂O)₂ was used instead of Nd(tta)₃(H₂O)₂. Yield: 35%. Anal. Calc. for C₆₆H₅₁F₉N₇O₆S₃ClIrGd (L_{Ir}-Gd(tta)₃·Et₃N·Cl): C, 46.86; H, 3.02; N, 5.80. Found: C, 46.23; H, 3.62; N, 5.94%.

L_{Ir2}-Nd(tta)₃: L_{Ir2}-Nd(tta)₃ was obtained by the similar procedure to L_{Ru2}-Nd(tta)₃ unless L_{Ir2}-Cl was used instead of L_{Ru2}-(PF₆)₂. Yield: 33%. Anal. Calc. for C₆₆H₄₇F₁₃N₇O₆S₃ClIrNd (L_{Ir2}-Nd(tta)₃·Et₃N·Cl): C, 45.32; H, 2.71; N, 5.61. Found: C, 44.56; H, 2.98; N, 5.57 %. ¹H-NMR (400 MHz, DMSO-*d*₆, 25 °C): δ = 8.21 (d, 2H), 7.89 (t, 2H), 7.70 (d, 2H), 7.58 (d, 2H), 7.18 (t, 2H), 7.12 (t, 2H), 6.98 (t, 2H), 6.91 (t, 2H), 6.07 (d, 2H), 5.84 (d, 2H). ¹³C NMR (400 MHz, DMSO-*d*₆, 25 °C): δ = 159.03, 157.33, 152.80, 152.60, 142.00, 138.06, 137.50, 128.34, 127.89, 126.03, 125.13, 124.62, 124.33, 115.54, 114.94.

L_{Ir2}-Yb(tta)₃: L_{Ir2}-Yb(tta)₃ was obtained by the similar procedure to L_{Ir2}-Nd(tta)₃ unless Yb(tta)₃(H₂O)₂ was used instead of Nd(tta)₃(H₂O)₂. Yield: 35%. Anal. Calc. for C₇₂H₆₂F₁₃N₈O₆S₃ClIrYb (L_{Ir2}-Yb(tta)₃·2Et₃N·Cl): C, 46.02; H, 3.33; N, 5.96. Found: C, 46.02; H, 2.95; N, 6.20%. ¹H-NMR (400 MHz, DMSO-*d*₆, 25 °C): δ = 8.21 (d, 2H), 7.90 (t, 2H), 7.71 (d, 2H), 7.58 (d, 2H), 7.37(s), 7.18 (t, 2H), 7.11 (t, 2H), 6.98 (t, 2H), 6.90 (t, 2H), 6.06 (d, 2H), 5.84 (d, 2H), 5.71(s), 5.30(s).

L_{Ir2}-Gd(tta)₃: L_{Ir2}-Gd(tta)₃ was obtained by the similar procedure

to L_{Ir2}-Nd(tta)₃ unless Gd(tta)₃(H₂O)₂ was used instead of Nd(tta)₃(H₂O)₂. Yield: 35%. Anal. Calc. for C₇₂H₆₂F₁₃N₈O₆S₃ClIrGd (L_{Ir2}-Gd(tta)₃·2Et₃N·Cl): C, 46.37; H, 3.33; N, 6.01. Found: C, 46.36; H, 2.86; N, 6.43%.



Scheme 2 Synthetic route of lanthanide complexes (Ln = Nd, Yb or Gd).

Results and discussion

The UV-vis absorption spectra of the Ru/Ir metalloligands and their Nd/Yb coordination complexes are shown in Fig. 1. As we can see, L_{Ru} metalloligand has multifold absorption bands, i.e., a strong and sharp peak around 290 nm originating from the $\pi \rightarrow \pi^*$ transition of bpy and BiBzIm ligands; a structured absorption bands with multiple peaks from 310 to 420 nm, bearing ILCT (intraligand charge transfer) character; and a long tail absorption band from 420 to 530 nm, which can be assigned to ¹MLCT (metal-to-ligand charge transfer) transitions from Ru^{II} metal center to ppy and BiBzIm organic ligands.²⁰

In comparison, the Nd/Yb complexes of L_{Ru} metalloligand also show the major UV absorption peak around 290 nm associating with ppy and BiBzIm and the broad absorption band extending beyond 550 nm contributed by the MLCT transitions of L_{Ru} metalloligand. Meanwhile, we can detect an obvious redshift for this MLCT absorption band due to lanthanide coordination. In addition, the originally structured ILCT absorption band around 300 to 400 nm was superimposed by a much stronger and sharper absorption peak centered at 350 nm. Based on the UV-vis absorption spectra of Ln(tta)₃(H₂O) shown in Fig. 1 inset, we can assign this band to the enol-form absorption of the tta ligands from Ln(tta)₃(H₂O) salts. Similar results are also observed in L_{Ru2} and its Nd/Yb coordination complexes. While for the two Ir(III) metalloligands and Nd/Yb coordination complexes, there are mainly two absorption peaks at 275 and 350 nm, attributed by $\pi \rightarrow \pi^*$ transitions from ppy, BiBzIm, and tta ligands. Comparatively, the MLCT transitions based on Ir(III) metalloligands are not so impressive, which extend in the range from 380 to 470 nm. This is in accordance with the general situation, in which the energies required for MLCT transitions are usually higher for Ir(III) than Ru(II) compounds with similar structures.

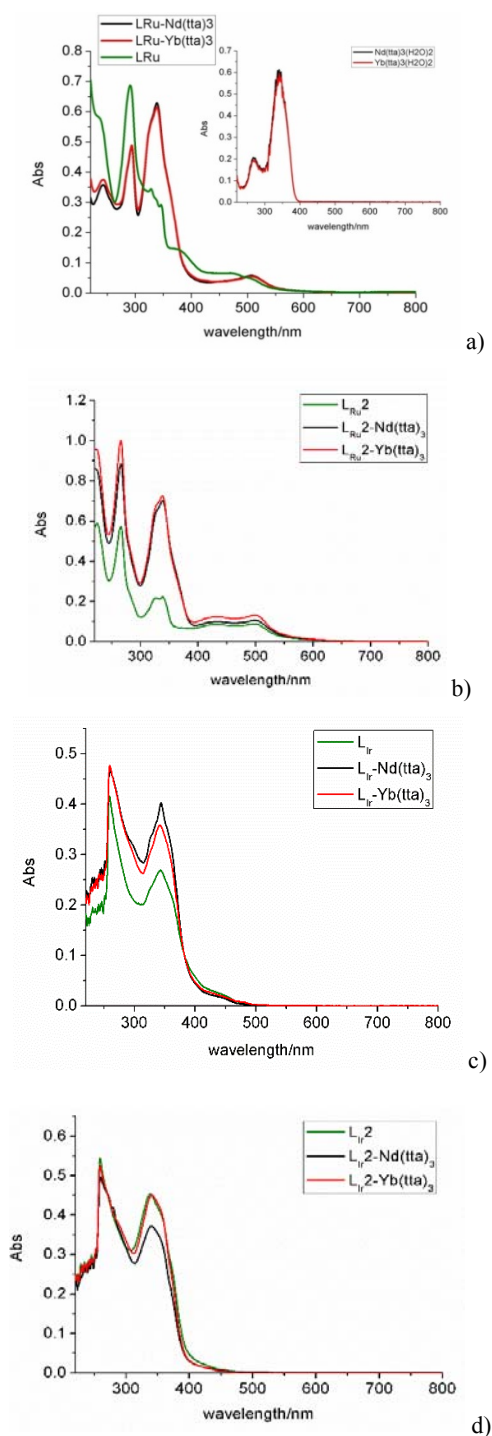


Fig. 1 The UV-vis absorption spectra of different Ru(II)/Ir(III) metalloligands and their Nd/Yb complexes. (a) L_{Ru} , (b) L_{Ru2} , (c) L_{Ir} , (d) L_{Ir2} .

The two Ru(II) metalloligands have wide excitation bands extending from 300 to 600 nm, and the excitation spectra detected for the two Ir(III) metalloligands cover 300 to 500 nm. As we can see in Fig. 2, L_{Ru} and L_{Ru2} show strong emission bands centered at 643 and 660 nm. And decay lifetime testing at room temperature (239 and 171 ns for L_{Ru} and L_{Ru2}) manifests the phosphorescent nature of the emission, originated from the 3MLCT excited levels of Ru(II) metalloligands. In comparison, the emissions of L_{Ir} and L_{Ir2} appear

in higher energy range, with maxima at 520 ($\tau = 47$ ns) and 523 nm ($\tau = 125$ ns), respectively. It is noted here that a well-structured profile can be detected in the emission of L_{Ir2} metalloligand at room temperature (also detectable in L_{Ir} , but less clearcut), which have also been observed in other literatures.²¹

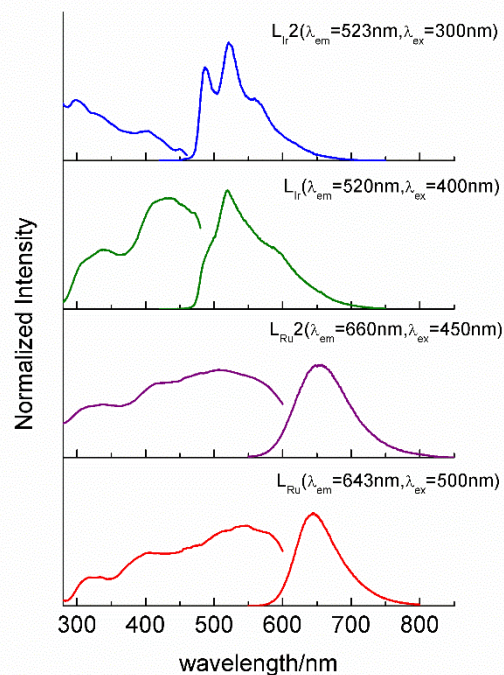


Fig. 2 Solid state emission of the Ru(II)/Ir(III) metalloligands measured at room temperature.

The designed Ru(II)/Ir(III) metalloligands can be applied to efficiently sensitize the excited states of NIR-emitting Nd^{3+} and Yb^{3+} ions, as estimated by the 3MLCT energy state from the phosphorescence data of their Gd-complexes. From Fig. 3, we can see that the emission profiles tested for the L_{Ru}/Ir -Gd compounds at room temperature and 77 K show little difference, but their decay lifetimes are obviously prolonged at low temperature (99, 135, 36, 66 ns at room temperature, and 177, 662, 683, 1095 ns at 77 K for L_{Ru} -Gd, L_{Ru2} -Gd, L_{Ir} -Gd, L_{Ir2} -Gd, respectively), in accordance with the general trend for phosphorescence emission from Ru(II)/Ir(III)-based complexes. Compared with their corresponding Ru(II)/Ir(III) metalloligands, the emissions are broadened in these Gd complexes and obvious redshift can also be detected in L_{Ru} -Gd and L_{Ru2} -Gd complexes, showing the coordination effect of Gd^{3+} . From the emission maxima, we calculated the 3MLCT energy state for the four metalloligands to be around 14, 286 (700 nm), 14, 184 (705 nm), 19, 230 (520 nm), and 20, 000 (500 nm) cm^{-1} , respectively, which are suitable for sensitizing the $^4F_{3/2}$ state of Nd^{3+} and $^2F_{5/2}$ state of Yb^{3+} energy levels situated at around 10,000 cm^{-1} . Therefore, for the Nd/Yb(III) coordination complexes assembled from the four metalloligands, the excitation into the Ru(II)/Ir(III) based MLCT transition resulted in the appearance of lanthanide-centered emissions occurring in the NIR region (Fig. 4). For Nd(III) complexes, there appear three emission peaks within 850-1500 nm: the main emission peak centered at 1061 nm ($^4F_{3/2} \rightarrow ^4I_{11/2}$), and two other peaks centered at 895 nm ($^4F_{3/2} \rightarrow ^4I_{9/2}$) and 1330 nm

($^4F_{3/2} \rightarrow ^4I_{13/2}$), respectively. While the Yb(III) complexes mainly show one broad emission band within 900-1080 nm, with a sharp peak protruded at 978 nm ($^2F_{5/2} \rightarrow ^2F_{7/2}$). It is also noticed from Fig. 4, that for Nd(III) complexes from L_{Ru} and L_{Ru2} metalloligands, the residual MLCT-based emission in the visible region is almost negligible, while that for Yb(III) complexes can be clearly detected within 500 to 700 nm. This shows that the energy transfer from Ru(II) metalloligands to Nd^{3+} is more efficient than to Yb^{3+} in these coordination complexes, and the quantum yield results (Table 1) based on decay lifetime tests are also in support of the above conclusion. As we can see, the quantum yield (ϕ_{Ln}) of the NIR emissions in Nd(III) complexes reaches 1%, while that for Yb(III) complexes is about 0.5%. In comparison, the quantum yields for Nd(III) complexes from the Ir(III) metalloligands are lower than their L_{Ru} (L_{Ru2}) counterparts, while the data for Yb(III) complexes are almost identical.

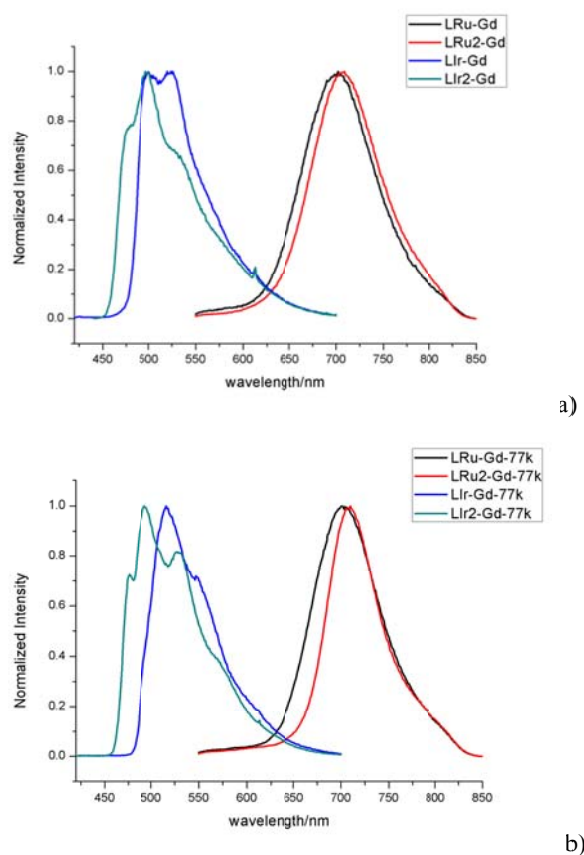


Fig. 3 Phosphorescence spectra of Gd(III) complexes from the Ru(II)/Ir(III) metalloligands at room temperature (a) and 77 K (b).

The decayed lifetime study of both MLCT and Ln(III)-based emissions clearly manifests the energy transfer process happened in the lanthanide coordination complexes based on Ru(II)/Ir(III) metalloligands. From the data summarized in Table 1 and using the energy transfer rate constant (k_{EnT}) equation $k_{EnT} = 1/\tau_q - 1/\tau_u$, in which τ_q refers to the “quenched” lifetime of Ru(II)/Ir(III) metalloligand (after coordination with Ln^{3+}) and τ_u refers to the “unquenched” lifetime (before coordination with Ln^{3+}), the Ru(II)/Ir(III)-Ln energy transfer rate for the Nd/Yb(III) complexes were estimated to be within 0.2 to $20 \times 10^7 s^{-1}$. Generally, Nd(III)

complexes have a faster energy transfer rate, which is due to the fact that Nd(III) has a higher density of $f \rightarrow f$ excited states between $10,000$ and $15,000 cm^{-1}$ compared with Yb(III) (Scheme 3), and can be a better energy acceptor from d -block Ru(II)/Ir(III) metalloligands. Especially, for complex L_{Ru} -Nd, the residual MLCT emission is almost totally quenched with the excitation of 450 nm, and the decayed lifetime is greatly reduced from the original 239 ns to 5 ns, amounting to a high energy transfer rate of $2 \times 10^8 s^{-1}$ from L_{Ru} metalloligand to Nd^{3+} ions. But we can also see that, a faster energy transfer rate from the metalloligand to Ln^{3+} ions does not definitely leads to a high quantum yield in lanthanide NIR emission (such as the case of L_{Ir} -Nd compared with L_{Ru2} -Nd), which might involve a more complicated energy transfer, migration, and dissipation process.

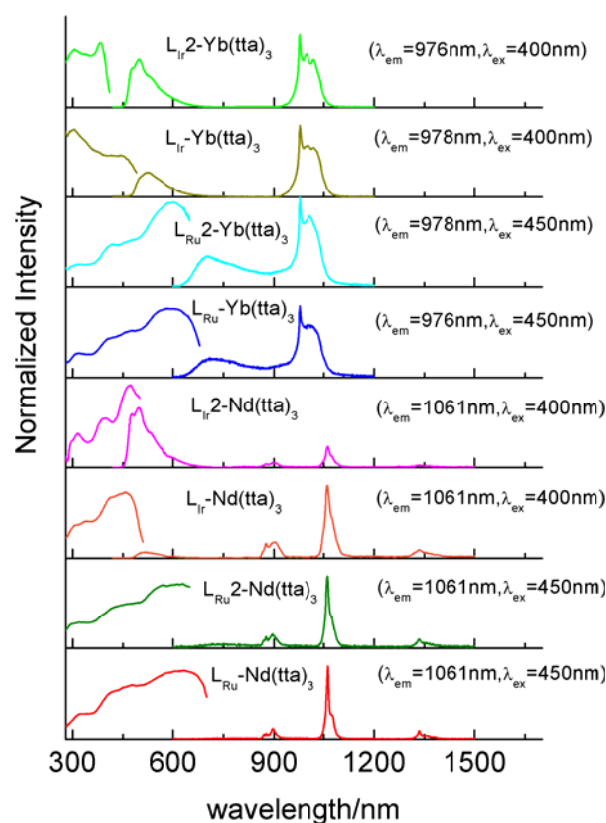


Fig. 4 Solid-state excitation and emission spectra of Nd/Yb(III) complexes from Ru(II)/Ir(III) metalloligands at room temperature.

Table 1 Photophysical data for MLCT-based visible emission and Ln(III)-based NIR emission in Ru(II)/Ir(III) metalloligands and their Nd/Yb(III) complexes.

	MLCT-based emission			Ln(III)-based emission		
	λ_{max}/nm	τ/ns	$k_{EnT}/10^7 s^{-1}$	λ_{max}/nm	$\tau/\mu s$	$\phi_{Ln}/\%$
L_{Ru}	643	239				
L_{Ru} -Nd	700	5	20	1061	2.56	1.0

L _{Ru} -Yb	700	77	0.9	976	9.08	0.5
L _{Ru2}	660	171				
L _{Ru2} -Nd	700	55	1.2	1061	2.34	0.9
L _{Ru2} -Yb	700	133	0.2	976	8.78	0.4
L _{Ir}	520	47				
L _{Ir} -Nd	518	10	8	1061	1.61	0.6
L _{Ir} -Yb	518	44	0.3	978	9.41	0.5
L _{Ir2}	523	125				
L _{Ir2} -Nd	500	25	3.2	1061	1.17	0.5
L _{Ir2} -Yb	500	31	2.4	976	8.58	0.4

k_{ET} (energy transfer rate constant) = $1/\tau_{\text{q}} - 1/\tau_{\text{u}}$ (τ_{q} and τ_{u} refer to the "quenched" and "unquenched" lifetime of Ru(II)/Ir(III) metalloligand before and after coordination with Ln³⁺). $\Phi_{\text{Ln}} = \tau/\tau_0$, in which τ_0 refers to the natural lifetime of Nd³⁺ (0.25 ms) or Yb³⁺ (2 ms).²²

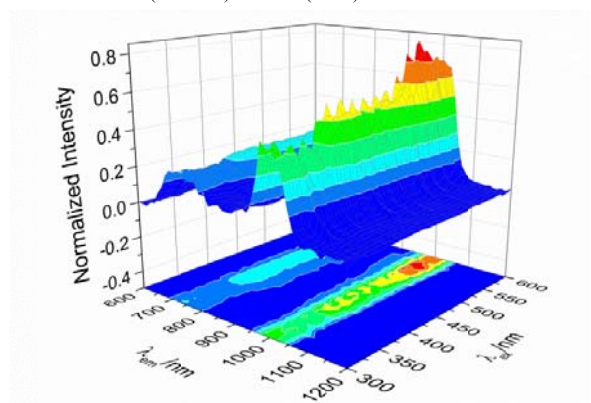
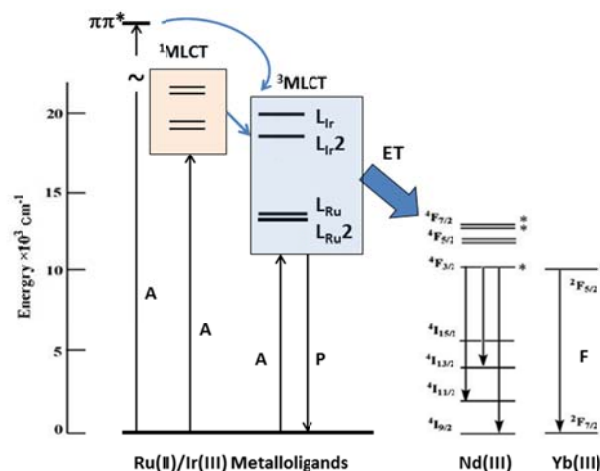


Fig. 5 Excitation-emission profile of L_{Ru}-Yb(III) complex.

The sensitization process from metalloligands to Ln(III) center was further examined by varying the excitation wavelength and observing the evolution of the NIR emissions of L_{Ru}-Yb(III) complex as an example (Fig. 5). We can see that although the NIR emissions of Yd³⁺ can be excited by steadily changing the excitation wavelengths from 300-600 nm, the most efficient sensitization was achieved upon excitation at the Ir(III)-based MLCT transitions from 450 to 550 nm in visible region. Summarizing the above results, we sketch the ET (energy transfer)-involved energy levels in the lanthanide complexes from Ru(II)/Ir(III) metalloligands in Scheme 3. As we can see, the ³MLCT energy levels of the four Ru(II)/Ir(III) metalloligands can transfer energy to the accepting excited levels of Nd³⁺ and Yb³⁺, which result in sensitized NIR emissions in these lanthanide complexes. And in comparison, the energy transfer efficiency is higher from Ru(II) ligands than Ir(III) ligands, since the energy states of the former match the energy states of Ln³⁺ ions better. For the two Ru(II) metalloligands, although organic functional group modification (phenanthroline vs. bipyridine) brings very slight energy difference in their ³MLCT energy levels, the energy transfer rates are greatly altered (see Table 1), and the final quantum efficiency of lanthanide NIR emission also shows some

difference. For Ir(III) metalloligands, the introduction of F-atoms leads to a higher ³MLCT energy state in L_{Ir2}, which makes the energy gap between ³MLCT and accepting levels of Ln(III) even larger. Therefore, both the energy transfer rates and quantum yields are lowered in L_{Ir2}-based complexes.



Scheme 3 Schematic energy transfer processes from Ru(II)/Ir(III) metalloligands to Nd³⁺ and Yb³⁺ (A=absorption, P=phosphorescence, F=fluorescence, ET=energy transfer).

Conclusions

In summary, we have designed four new Ru(II)/Ir(III) metalloligands by the method of organic functional group modification. And a series of d-f heteronuclear assemblies are obtained from the coordination of these metalloligands with Yb(III) and Nd(III) lanthanide ions. The Ru(II)/Ir(III) metalloligands show strong visible light ³MLCT emission by themselves, but upon coordination, the ³MLCT emissions are quenched to some extent and sensitize the Ln(III)-based NIR emissions by efficient d→f energy transfer. Both the energy transfer rates and lanthanide NIR luminescent quantum yields can be influenced by modification in the metalloligands. Especially, L_{Ru} presents the most efficient candidate for visible light harvesting antenna in sensitizing Nd(III)-based NIR luminescence.

Acknowledgements

This work was supported by the NSFC Projects (91222201, 21373276, 21450110063), the NSF of Guangdong Province (S2013030013474), the Fundamental Research Funds for the Central Universities (15lgzd05), and the RFDP of Higher Education of China for funding.

Notes and references

^a MOE Laboratory of Bioinorganic and Synthetic Chemistry, State Key Laboratory of Optoelectronic Materials and Technologies, School of Chemistry and Chemical Engineering, Sun Yat-Sen University, Guangzhou 510275, China

panm@mail.sysu.edu.cn; shaog@mail.sysu.edu.cn;
cesscy@mail.sysu.edu.cn

^b State Key Laboratory of Structural Chemistry, Fujian Institute of Research on the Structure of Matter, Chinese Academy of Sciences, Fuzhou 350002, China

^c State Key Laboratory of Organometallic Chemistry, Shanghai Institute of Organic Chemistry, Chinese Academy of Sciences, Shanghai 200032, China

1. O. S. Wolbeis, *Lanthanide Luminescence*, Springer, New York, 2011.
2. (a) H. S. Jang, H. Yang, S. W. Kim, J. Y. Han, S. G. Lee and D. Y. Jeon, *Adv. Mater.*, 2008, **20**, 2696; (b) F. Wang, R. Deng, J. Wang, Q. Wang, Y. Han, H. Zhu, X. Chen and X. Liu, *Nat. Mater.*, 2011, **10**, 968.
3. (a) S. K. Singh, A. K. Singh and S. B. Rai, *Nanotechnology*, 2011, **22**, 275703; (b) F. Wang, D. Banerjee, Y. Liu, X. Chen and X. Liu, *Analyst*, 2010, **135**, 1839; (c) Y. Liu, D. Tu, H. Zhu, R. Li, W. Luo and X. Chen, *Adv. Mater.*, 2010, **22**, 3266.
4. (a) F. Wang, X. Liu, *Chem. Soc. Rev.*, 2009, **38**, 976; (b) M. Haase, H. Schäfer, *Angew. Chem.*, 2011, **123**, 5928; *Angew. Chem. Int. Ed.*, 2011, **50**, 5808; (c) X. Li, F. Zhang, D. Zhao, *Nano Today*, 2013, **8**, 643.
5. (a) F. C. J. M. van Veggel, C. Dong, N. J. J. Johnson, J. Pichaandi, *Nanoscale*, 2012, **4**, 7309; (b) Y. Zhang, L. Zhang, R. Deng, J. Tian, Y. Zong, D. Jin, X. Liu, *J. Am. Chem. Soc.*, 2014, **136**, 4893; (c) D. Tu, L. Liu, Q. Ju, Y. Liu, H. Zhu, R. Li and X. Chen, *Angew. Chem.*, 2011, **123**, 6430.
6. (a) N. M. Shavaleev, R. Scopelliti, F. Gumy, and J.C. G. Bünzli, *Inorg. Chem.*, 2009, **48**, 2908; (b) C. Doffek, N. Alzakhem, M. Molon, and M. Seitz, *Inorg. Chem.*, 2012, **51**, 4539; (c) W. Huang, D. Wu, D. Guo, X. Zhu, C. He, Q. Meng and C. Duan, *Dalton Trans.*, 2009, 2081.
7. (a) Y. Liu, M. Pan, Q.-Y. Yang, L. Fu, K. Li, S.-C. Wei, and C.-Y. Su, *Chem. Mater.*, 2012, **24**, 1954; (b) M. Pan, X.-L. Zheng, Y. Liu, W.-S. Liu and C.-Y. Su, *Dalton Trans.*, 2009, 2157; (c) Q.-Y. Yang, K. Wu, J.-J. Jiang, C.-W. Hsu, M. Pan, J.-M. Lehn and C.-Y. Su, *Chem. Commun.*, 2014, **50**, 7702; (d) Q.-Y. Yang, M. Pan, S.-C. Wei, C.-W. Hsu, J.-M. Lehn, and C.-Y. Su, *CrystEngComm*, 2014, **16**, 6469.
8. (a) F. Artizzu, M. Laura Mercuri, A. Serpe, P. Deplano, *Coord. Chem. Rev.*, 2011, **255**, 2514; (b) J. Feng, H. J. Zhang, *Chem. Soc. Rev.*, 2013, **42**, 387; (c) J. M. Stanley, B. J. Holliday, *Coord. Chem. Rev.*, 2012, **256**, 1520; (d) M. D. Ward, *Coord. Chem. Rev.*, 2007, **251**, 1663; (e) J.-C. G. Bünzli and C. Piguet, *Chem. Soc. Rev.*, 2005, **34**, 1048; (f) J. Kido, Y. Okamoto, *Chem. Rev.*, 2002, **102**, 2357.
9. (a) J. Yu, L. Zhou, H. Zhang, Y. Zheng, H. Li, R. Deng, Z. Peng and Z. Li, *Inorg. Chem.*, 2005, **44**, 1611; (b) F. Liang, Q. Zhou, Y. Cheng, L. Wang, D. Ma, X. Jing and F. Wang, *Chem. Mater.*, 2003, **15**, 1935; (c) K. Hanaoka, K. Kikuchi, S. Kobayashi, and T. Nagano, *J. Am. Chem. Soc.*, 2007, **129**, 13502.
10. (a) R. V. Deun, P. Fias, P. Nockemann, K. V. Hecke, L. V. Meervelt, and K. Binnemans, *Inorg. Chem.*, 2006, **45**, 10416; (b) L. Sun, Y. Qiu, T. Liu, H. Peng, W. Deng, Z. Wang, and L. Shi, *RSC Adv.*, 2013, **3**, 26367.
11. (a) L. Li, S. Zhang, L. Xu, Z.-N. Chen and J. Luo, *J. Mater. Chem. C*, 2014, **2**, 1698; (b) A. M. Nonat, C. Allain, S. Faulkner, and T. Gunnlaugsson, *Inorg. Chem.*, 2010, **49**, 8449.
12. (a) L. Aboshyan-Sorgho, H. Nozary, A. Aebischer, J. C. G. Bünzli, P. Y. Morgantini, K. R. Kittilstved, A. Hauser, S. V. Eliseeva, S. Petoud and C. Piguet, *J. Am. Chem. Soc.*, 2012, **134**, 12675; (b) J. Li, J. Y. Wang and Z. N. Chen, *J. Mater. Chem. C*, 2013, **1**, 3661; (c) R. M. Edkins, D. Sykes, A. Beeby, M. D. Ward, *Chem. Commun.*, 2012, **48**, 9977.
13. (a) L. J. Charbonnière, S. Faulkner, C. Platas-Iglesias, M. Regueiro-Figueroa, A. Nonat, T. Rodríguez-Blas, A. de Blas, W. S. Perryd, M. Tropicano, *Dalton Trans.*, 2013, **42**, 3667; (b) M. Tropicano, C. J. Record, E. Morris, H. S. Rai, C. Allain, S. Faulkner, *Organometallics*, 2012, **31**, 5673; (c) E. D. Piazza, L. Norel, K. Costuas, A. Bourdolle, O. Maury, S. Rigaut, *J. Am. Chem. Soc.*, 2011, **133**, 6174.
14. (a) S. J. A. Pope, B. J. Coe, S. Faulkner, E. V. Bichenkova, X. Yu and K. T. Douglas, *J. Am. Chem. Soc.*, 2004, **126**, 9490; (b) L. N. Li, S. Q. Zhang, L. J. Xu, L. Han, Z. N. Chen and J. H. Luo, *Inorg. Chem.*, 2013, **52**, 12323.
15. (a) J. An, C. M. Shade, D. A. Chengelis-Czegán, S. Petoud, N. L. Rosi, *J. Am. Chem. Soc.*, 2011, **133**, 1220; (b) D. J. Lewis, P. B. Glover, M. C. Solomons, and Z. Pikramenou, *J. Am. Chem. Soc.*, 2011, **133**, 1033; (c) A. de Bettencourt-Dias, P. S. Barber, and S. Bauer, *J. Am. Chem. Soc.*, 2012, **134**, 6987.
16. (a) S. Pandya, J. Yu, D. Parker, *Dalton Trans.*, 2006, 2757; (b) S. V. Eliseeva, J.-C. G. Bünzli, *Chem. Soc. Rev.*, 2010, **39**, 189; (c) J.-C. G. Bünzli, *Chem. Rev.*, 2010, **110**, 2729.
17. (a) N. M. Shavaleev, G. Accorsi, D. Virgili, Z. R. Bell, T. Lazarides, G. Calogero, N. Armaroli, and M. D. Ward, *Inorg. Chem.*, 2005, **44**, 61; (b) N. M. Shavaleev, L. P. Moorcraft, S. J. A. Pope, Z. R. Bell, S. Faulkner, and M. D. Ward, *Chem. Eur. J.*, 2003, **9**, 5283; (c) Q.-H. Wei, Y.-F. Lei, W.-R. Xu, J.-M. Xie, G.-N. Chen, *Dalton Trans.*, 2012, **41**, 11219.
18. (a) Q. Zhao, C. H. Huang and F. Y. Li, *Chem. Soc. Rev.*, 2011, **40**, 2508; (b) M. X. Yu, Q. Zhao, L. X. Shi, F. Y. Li, Z. G. Zhou, H. Yang, T. Yi and C. H. Huang, *Chem. Commun.*, 2008, 2115.
19. A. J. Hallett, B. M. Kariuki and S. J. A. Pope, *Dalton Trans.*, 2011, **40**, 9474.
20. K. K.-W. Lo, K. Y. Zhang, S.-K. Leung, and M.-C. Tang, *Angew. Chem. Int. Ed.*, 2008, **47**, 2213.
21. (a) S. Singaravadivel, E. Babu, M. Velayudham, K. L. Lu, S. Rajagopal, *J. Organomet. Chem.*, 2013, **738**, 49; (b) T. Lazarides, N. M. Tart, D. Sykes, S. Faulkner, A. Barbieri and M. D. Ward, *Dalton Trans.*, 2009, 3971; (c) P. Coppo, M. Duati, V. N. Kozhevnikov, J. W. Hofstraat, and L. De Cola, *Angew. Chem. Int. Ed.*, 2005, **44**, 1806.